

Pregabalin Mediates Retinal Ganglion Cell Survival From Retinal Ischemia/Reperfusion Injury Via the Akt/GSK3 β /β-Catenin Signaling Pathway

Jing Xu,¹ Yuyan Guo,¹ Qiong Liu,¹ Hui Yang,² Ming Ma,¹ Jian Yu,¹ Linjiang Chen,¹ Chunlian Ou,³ Xiaohui Liu,⁴ and Jing Wu⁵

¹Department of Ophthalmology, Nanfang Hospital, Southern Medical University, Guangzhou, Guangdong, China

²State Key Laboratory of Ophthalmology, Zhongshan Ophthalmic Center, Sun Yat-sen University, Guangzhou, Guangdong, China

³Department of General Practice, Nanfang Hospital, Southern Medical University, Guangzhou, Guangdong, China

⁴Department of Ophthalmology, The Second People's Hospital of Foshan, Foshan, Guangdong, China

⁵Huiqiao Medical Center, Nanfang Hospital, Southern Medical University, Guangzhou, Guangdong, China

Correspondence: Jing Wu, Huiqiao Medical Center, Nanfang Hospital, Southern Medical University, Guangzhou 510515, Guangdong, China;
wujingsci@126.com.

Xiaohui Liu, Department of Ophthalmology, The Second People's Hospital of Foshan, Foshan 528000, Guangdong, China;
xiaohuihui1208@163.com.

JX and YG contributed equally to the work presented here and should therefore be regarded as equivalent authors.

Received: April 14, 2022

Accepted: October 10, 2022

Published: November 3, 2022

Citation: Xu J, Guo Y, Liu Q, et al. Pregabalin mediates retinal ganglion cell survival from retinal ischemia/reperfusion injury via the Akt/GSK3 β /β-catenin signaling pathway. *Invest Ophthalmol Vis Sci*. 2022;63(12):7.

<https://doi.org/10.1167/iovs.63.12.7>

PURPOSE. Progressive retinal ganglion cell (RGC) loss induced by retinal ischemia/reperfusion (RIR) injury leads to irreversible visual impairment. Pregabalin (PGB) is a promising drug for neurodegenerative diseases. However, with regard to RGC survival, its specific role and exact mechanism after RIR injury remain unclear. In this study, we sought to investigate whether PGB could protect RGCs from mitochondria-related apoptosis induced by RIR and explore the possible mechanisms.

METHODS. C57BL/6J mice and primary RGCs were pretreated with PGB prior to ischemia/reperfusion modeling. The retinal structure and cell morphology were assessed by immunochemical assays and optical coherence tomography. CCK8 was used to assay cell viability, and an electroretinogram was performed to detect RGC function. Mitochondrial damage was assessed by a reactive oxygen species (ROS) assay kit and transmission electron microscopy. Western blot and immunofluorescence assays quantified the expression of proteins associated with the Akt/GSK3 β /β-catenin pathway.

RESULTS. Treatment with PGB increased the viability of RGCs in vitro. Consistently, PGB preserved the normal thickness of the retina, upregulated Bcl-2, reduced the ratio of cleaved caspase-3/caspase-3 and the expression of Bax in vivo. Meanwhile, PGB improved mitochondrial structure and prevented excessive ROS production. Moreover, PGB restored the amplitudes of oscillatory potentials and photopic negative responses following RIR. The mechanisms underlying its neuroprotective effects were attributed to upregulation of the Akt/GSK3 β /β-catenin pathway. However, PGB-mediated neuroprotection was suppressed when using MK2206 (an Akt inhibitor), whereas it was preserved when treated with TWS119 (a GSK3 β inhibitor).

CONCLUSIONS. PGB exerts a protective effect against RGC apoptosis induced by RIR injury, mediated by the Akt/GSK3 β /β-catenin pathway.

Keywords: retinal ischemia/reperfusion, retinal ganglion cell, Akt/GSK3 β /β-catenin

Glaucoma refers to a group of eye diseases characterized by idiopathic optic nerve injury, predicted to affect over 100 million people worldwide by 2040.¹ Angle-closure glaucoma is a form of glaucoma with high incidence in Asia, often presenting with acute loss of vision, pain, and high intraocular pressure (IOP).¹ Retinal ischemia/reperfusion (RIR) injury is triggered by transient intraocular hypertension, the main risk factor for glaucoma, leading to the death of retinal ganglion cells (RGCs) and irreversible visual impairment.^{2,3} RGCs are the output cells required for visual signal transmission from the retina into the brain, and their loss contributes to permanent retinal neurological deficits.⁴ The exact pathogenesis of RGC death remains largely unclear. An increasing body of evidence suggests

that mitochondrial dysfunction and excessive accumulation of reactive oxygen species (ROS) caused by oxidative stress is critical for the apoptosis of RGCs.^{5–9} However, currently available approaches that lower IOP via surgery or medication cannot effectively prevent progressive RGC death and visual field defects in patients with glaucoma.¹⁰ Therefore, alternative antioxidation-based strategies aiming to achieve neuroprotection are warranted. Pregabalin (PGB) is a structural derivative of gamma-aminobutyric acid that has been widely used as an analgesic for diabetic peripheral neuropathy.¹¹ Current evidence suggests that PGB can bind to the α_2 - δ subunit of the voltage-dependent calcium channels at the presynaptic membrane of neurons. By effectively blocking the voltage-gated calcium channels, PGB significantly



reduces the inflow of calcium ions, thereby inhibiting the release of excitatory neurotransmitters such as glutamate and stabilizing nerve cells.^{12–14} Besides its well-known therapeutic spectrum, it was recently found to exert a neuroprotective effect against diabetic retinopathy by suppressing retinal glutamate, glial cell activation, and the inflammatory burden.¹⁵ However, the detailed mechanisms and the effects of PGB on RGC survival after RIR injury remain unclear.

The present study investigated whether PGB could protect RGCs from RIR insult and explored the underlying mechanisms. Results showed that PGB enhanced RGC recovery from RIR by suppressing ROS production and subsequent mitochondria-driven RGC apoptosis in the retina. The mechanisms underlying its neuroprotective effects were attributed to upregulation of the Akt/GSK3 β /β-catenin pathway, which contributed to alleviation of RGC apoptosis. Collectively, our data provide novel insights into the mechanisms of RIR-mediated injury and demonstrate that PGB has great prospects for application, given its neuroprotective potential to prevent RGC death during glaucoma.

METHODS

Animals

Male mice were used in the experiments to avoid the neuroprotective effect of ovarian hormones.¹⁶ Eight-week-old C57BL/6J male mice were obtained from the animal center of Southern Medical University (Guangzhou, China). All experimental procedures were approved by the Institutional Animal Care and Use Committee of Southern Medical University (Guangzhou, China) and performed according to the ARVO Statement for the Use of Animals in Ophthalmic and Vision Research.

Establishment of the RIR Model

Adult male mice were anesthetized by an intraperitoneal injection of 50 mg/kg pentobarbital sodium. Before the operation, 1% tropicamide eye drops (Santen Pharmaceutical Co., Ltd., Osaka, Japan) were used to dilate the pupils, and 0.5% ropivacaine hydrochloride (Santen Pharmaceutical) was used for corneal anesthesia. Then, a 33-gauge needle connected to a saline solution was inserted into the anterior chamber in a single pass to stabilize the IOP between 110 and 120 mm Hg for 60 minutes. The animal model was evaluated by monitoring IOP and retinal vessel color. IOP was measured as previously described by Chen et al.¹⁷ (Supplementary Data S1), and retinal ischemia was confirmed by microscopy (Supplementary Data S2). The RIR model was performed in only one eye for each mouse, and the contralateral eye was untreated. A sham procedure was performed in a separate group with cannulation of one eye without elevating the pressure (Supplementary Data S3). Carbomer eye drops (Bausch + Lomb, Bridgewater, NJ, USA) were used to moisten the eyes during ischemic injury. After 60 minutes of retinal ischemia, the needle was carefully withdrawn to normalize the IOP and restore retinal vascular perfusion, and ofloxacin ointment (Santen Pharmaceutical) was applied to the experimental eye to prevent bacterial infection.

Pharmacological Treatment

According to the random number table, mice were divided into five groups: control ($n = 42$), NaCl ($n = 42$), 15 mg/kg PGB ($n = 18$; Pfizer, New York, NY, USA), 30 mg/kg PGB ($n = 42$), and 60 mg/kg PGB ($n = 18$). (The number of mice in each experiment is shown in Supplementary Data S4.) Mice in the NaCl and PGB groups were subjected to experimental RIR. Mice in the NaCl and PGB groups received intraperitoneal injections of 1 mL NaCl or PGB solution, respectively, 48 hours, 24 hours, and 0.5 hour before the onset of operation.

Optical Coherence Tomography Imaging

The retinal nerve fiber layer (RNFL) and ganglion cell complex (GCC) were longitudinally measured in live mice on day 7 after RIR using noninvasive high-resolution spectral-domain optical coherence tomography (SD-OCT; Heidelberg Engineering, Heidelberg, Germany). After corneal edema subsided (Supplementary Data S5), OCT tests were conducted. Mice were anesthetized and pupils were dilated. For each eye, the average and fan-shaped (upper, lower, nasal, and temporal) RNFL and GCC around the optic papilla were determined by a circular B-scan with the optic nerve head as the center. At least three scans with signal quality greater than 20 dB were performed for each eye. The scanned images were automatically processed by built-in software to segment the retina layer and quantify thickness values. The segmentation quality was independently checked by two trained observers blinded to the grouping and treatment conditions. Samples were manually corrected to include only the RNFL or GCC.

Quantification of RGCs

Mice were killed by an overdose of anesthesia, and the retinas were harvested and fixed in 4% paraformaldehyde. Next, they were placed in goat serum with 0.5% Triton X-100 for 1 hour and then incubated in mouse-anti-Brn3a antibody (1:100, sc-8429; Santa Cruz Biotechnology, Dallas, TX, USA) overnight at 4°C. After several washes the next day, retinas were incubated with goat anti-mouse IgG secondary antibody conjugated to Alexa Fluor 488 (1:200, E032210; EarthOx, Burlingame, CA, USA) for 1 hour at room temperature. Retinas were then flatmounted on glass slides, divided into four quadrants, and coverslipped. We used a fluorescence microscope to acquire three images of 0.3588 mm² at intervals of 1 mm in each quadrant representing the peripheral, medial, and central retinas. Survival of RGCs was determined by counting the number of Brn3a-positive cells in each separate region of the flat whole-mount retina using Image J software (National Institutes of Health, Bethesda, MD, USA) and obtaining the average value.

Western Blot

Total protein was isolated from the retinal samples and run on 10% polyacrylamide gels following a standard protocol. Equal amounts of protein resolved by polyacrylamide gels were immunoblotted using antibodies against β-tubulin (1:10000, RM2003; Beijing Ray Antibody Biotech, Beijing, China), glyceraldehyde-3-phosphate dehydrogenase (GAPDH, 1:10,000, RM2002; Beijing Ray Antibody Biotech), caspase-3 (1:1000, 9662; Cell Signaling Technology, Danvers, MA, USA), Bax (1:1000, 2772; Cell Signaling Technology),

B-cell lymphoma-2 (Bcl-2; 1:1000, ab182858; Abcam, Cambridge, UK), Akt (1:1000, YT0177; ImmunoWay, Plano, TX, USA), phosphorylated Akt (p-Akt; 1:1000, YP0006; ImmunoWay), glycogen synthase kinase-3 beta (GSK3 β ; 1:1000, 12456; Cell Signaling Technology), phosphorylated GSK3 β (p-GSK3 β ; 1:1000, 9323; Cell Signaling Technology), and β -catenin (1:1000, ab32572; Abcam). They were then detected with a chemiluminescence kit. Gray value analysis was conducted using Image J software.

Histology and Staining of Retinal Sections

Mouse eyes were harvested and embedded in paraffin, and 4- μ m-thick sections were obtained from each paraffin block. Three slices were prepared for each eye and stained with hematoxylin and eosin (H&E). Then, a fluorescence microscope (BX63; Olympus, Tokyo, Japan) was used to take retinal images, and the whole retinal thickness was measured at 500 μ m from the center of the optic disk by Image J software. The data obtained from three sections per eye were averaged.

For cryosectioning and immunofluorescence (IF) studies, animals were deeply anesthetized and intracardially perfused with 0.9% normal saline, followed by 4% paraformaldehyde. Each eye was post-fixed and dehydrated, the samples were embedded in an optimal cutting temperature compound, and transverse cryosections of thickness 6 μ m were obtained by a microtome (Leica, Wetzlar, Germany). IF detection was carried out using antibodies against p-Akt, p-GSK3 β , and β -catenin. Images were captured over regions 350 μ m in length at a distance of 300 μ m from the center of the optic nerve in radial retinal sections by a fluorescence microscope and processed by Image-Pro Plus 6.0 (Media Cybernetics, Rockville, MD, USA). Three slices per eye were analyzed, and the number of positive cells (Brn3a $^+$ and p-Akt $^+$ /p-GSK3 β $^+$ / β -catenin $^+$) was counted in the entire retinal section and normalized to the length of the respective section. The positivity rate was presented as the percentage of the ratio between the experimental and the control eye.¹⁸ The investigator was blinded to the grouping when performing the experiment and extracting data. All data were analyzed by an operator blinded to the grouping strategy.

TUNEL Staining Assay

The apoptosis of RGCs was assessed using the In Situ Cell Death Detection Kit, Fluorescein (11684795910; Roche Pharma, Basel, Switzerland), according to the manufacturer's protocol. Both 4',6'-diamidino-2-phenylindole (DAPI, BB-4401; BestBio, Shanghai, China) and Brn3a (primary antibody: Anti-Brn3a/BRN3A/POU4F1 Antibody, sc-8429; Santa Cruz Biotechnology; secondary antibody: Invitrogen Alexa Fluor 594 Donkey anti-Mouse, A-21203; Thermo Fisher Scientific, Waltham, MA, USA) staining was performed as described previously. Photographs were captured using the BX63 fluorescence microscope and analyzed by a blinded investigator. Three slices per eye were analyzed from each sample. TUNEL $^+$ /Brn3a $^+$ and TUNEL $^-$ /Brn3a $^+$ cells were regarded as apoptotic and surviving RGCs, respectively.

Transmission Electron Microscopy

The dissected retina was fixed in phosphate-buffered 2.5% glutaraldehyde and 1% osmic acid solution followed

by dehydration and was then placed in the embedding solution. Then, 50-nm-thick sections of the retina were obtained, carefully mounted on copper grids, stained with uranyl acetate and lead citrate, and examined under a transmission electron microscope (Hitachi, Tokyo, Japan).

Electroretinogram

Before electroretinogram (ERG) recording, mice were subjected to dark adaptation for 14 hours. During ERG recording, the gold-plated wire loop, which was in contact with the corneal surface, served as the active electrode, and the stainless-steel needle electrodes inserted between the two ears and in the caudal skin served as the reference and ground leads, respectively. Animals were first exposed to white flashes with increasing intensities ranging from 0.001 to 10.0 cd·s/m 2 under dark adaptation, and scotopic responses were recorded. Then animals were light adapted for 10 minutes with a white background (25 cd /m 2), and photopic responses to white flashes of 3.0 cd·s/m 2 and 10.0 cd·s/m 2 were recorded. For each condition (scotopic and photopic), three to 10 responses were elicited by luminance flash stimuli, with the stimulus interval varying from 2 to 10 seconds at low intensities to 1 minute at intensities above 3.0 cd·s/m 2 . The ERG data were collected by an amplifier of the RETIscan system (Roland Consult Electrophysiology and Imaging, Brandenburg an der Havel, Germany) at a sampling rate of 2 kHz and analyzed with RETIport software after 50-Hz low-pass filtering. To isolate the oscillatory potentials (OPs) recorded at scotopic 3.0 cd·s/m 2 , a 100- to 300-Hz bandpass filter was applied instead of a 50-Hz low-pass filter. To analyze the ERG waveform, the a-wave amplitude was measured from baseline to the first negative peak, and the b-wave amplitude was measured from the a-wave trough to the next positive peak. The photopic negative response (PhNR) was measured as the amplitude of the first negative peak following the b-wave relative to the baseline. To measure the amplitude of OPs, the peak-to-peak amplitudes of four major peaks were measured and then averaged.

GSK3 β Activity Assay

GSK3 β activity in retinal lysates was measured using the Tissue GSK3 β Kinase Activity Spectrometry Quantitative Detection Kit (GenMed, Plymouth, MN, USA) according to the manufacturer's instructions. GSK3 β activity was detected at an absorbance of 340 nm.

Primary Culture of RGCs

According to the protocol of Winzeler and Wang,¹⁹ retinal cells were quickly isolated from the retina of P3 neonatal mice and incubated in goat-anti-mouse macrophage antibody-coated flasks (Jackson ImmunoResearch, West Grove, PA, USA) to remove adherent macrophages. Non-adherent cells were then transferred to CD90 monoclonal antibody-coated flasks (Bio-Rad Laboratories, Hercules, CA, USA) to collect adherent RGCs. The isolated RGCs were incubated in a growth medium containing supplements at 37°C in 5% CO $_2$.

Oxygen–Glucose Deprivation and Reoxygenation

RGCs were washed with PBS twice, and the medium was replaced with glucose-free Dulbecco's Modified Eagle's Medium (DMEM). The cells were then transferred to an anoxia incubator (Shel Lab, Cornelius, OR, USA) filled with 95% N₂ and 5% CO₂ for 3 hours. The control groups were cultured with DMEM containing glucose in an aerobic environment (95% air and 5% CO₂) for the same duration. At the end of the oxygen–glucose deprivation (OGD) period, all groups were returned to an aerobic environment (95% air and 5% CO₂) and were incubated for 12 hours, and the medium was replaced with DMEM containing glucose.²⁰

Cell Viability

Cell viability was detected using the CCK8 kit (Dojindo Laboratories, Kumamoto, Japan). After OGD/reoxygenation (R) treatment, RGCs were cultured with 20 μL CCK8 and 180 μL medium in each well at 37°C for 4 hours. Moreover, the absorbance at 450 nm was measured using a multi-functional microplate reader (Molecular Devices, San Jose, CA, USA).

ROS Assay

ROS levels were quantified using a ROS Assay Kit (Beyotime Biotech, Jiangsu, China). Briefly, primary RGCs or single-cell suspensions from the retina were incubated with 10-μM dichloro-dihydro-fluorescein diacetate (DCFH-DA) at 37°C for 20 minutes. Then, the samples were washed with PBS, and the fluorescent intensity was detected by an inverted fluorescence microscope (IX73; Olympus) and flow cytometry (BD Biosciences, San Jose, CA, USA). Data were analyzed using ImageJ and FlowJo software. An inverted fluorescence microscope detected the fluorescence at an excitation wavelength of 488 nm, and ROS levels were defined as the proportion of green cells. All photographs were taken and data analyzed by operators blinded to the treatment groups.

Statistical Analysis

The data are expressed as mean ± SEM. One-way ANOVA was performed, followed by Tukey's post hoc test using SPSS Statistics 20.0 (IBM, Chicago, IL, USA). All statistical tests were two tailed, and *P* values below 0.05 were statistically significant.

RESULTS

Neuroprotective Effects of PGB After RIR Injury

Immediately after the IOP was increased, fundal examination under the microscope revealed blanching of retinal blood flow and whitening of the entire retina. The retina regained its original color when the needle was removed from the anterior chamber (Fig. 1A). Meanwhile, we evaluated IOP changes during RIR (Supplementary Data S1). These results indicate successful establishment of the RIR model.

To evaluate the neuroprotective role of PGB in RIR, PGB was administered intraperitoneally before surgery (Fig. 1B). Seven days after reperfusion, the thickness of the whole

retina exposed to RIR in H&E staining decreased by 53.42 ± 3.37 μm. However, retinal damage was significantly ameliorated by PGB, with thickness increases of 16.67 ± 3.31 μm, 40.17 ± 3.51 μm, and 21.88 ± 4.33 μm after pretreatment with 15 mg/kg, 30 mg/kg, and 60 mg/kg PGB,^{21–23} respectively (Figs. 1C, 1F). Similar results were observed in the whole retina thickness during OCT (Supplementary Data S6A). Changes in the thickness of RNFL and GCC monitored by OCT demonstrated the neuroprotective effect of PGB in RIR, with a decreased thickness of 6.86 ± 0.75 μm for RNFL and 28.00 ± 8.08 μm for GCC after RIR. After pretreatment with 30 mg/kg PGB, RNFL thickness significantly increased by 6.91 ± 0.79 μm and GCC thickness by 29.57 ± 8.10 μm (Figs. 1D, 1F). Immunostaining of the whole-mount retina for Brn3a showed that the number of RGCs in the experimental mice decreased by 1072.00 ± 80.89/0.3588 mm² 7 days after reperfusion. PGB pretreatment rescued RGC death, compared to the control group, with increases of 164.30 ± 49.00/0.3588 mm² and 308.30 ± 19.84/0.3588 mm² at 15 mg/kg and 30 mg/kg, respectively (Figs. 1E, 1F). These data indicate that treatment with PGB confers a neuroprotective effect against RIR in the retina in a dose-dependent manner at 15 and 30 mg/kg. However, the toxicity of PGB was observed at a higher concentration.

Influence of PGB on the Mitochondrial Apoptotic Pathway

It is widely acknowledged that PGB has anti-apoptotic properties. To further investigate the potential mechanism, we detected the expression of the Bcl-2 family and caspase family, which play pivotal roles in mitochondria-dependent apoptosis. PGB pretreatment decreased the density of pro-apoptotic protein Bax but increased the density of anti-apoptotic protein Bcl-2 (Fig. 2A). Meanwhile, PGB reversed the elevation of cleaved caspase-3 initially induced by RIR (Fig. 2B), indicating that PGB could protect the retina against RIR-induced mitochondrial apoptosis, with the most pronounced effect at 30 mg/kg with a good safety profile (Supplementary Data S7). Accordingly, 30 mg/kg PGB was selected for further experiments.

Current evidence suggests that the mitochondrial apoptosis pathway can be triggered by ROS, which induces intracellular oxidative stress.²⁴ Flow cytometry of the FITC⁺ RGCs showed that ROS was increased after RIR injury compared to the control group. Additionally, PGB pretreatment significantly inhibited ROS generation, indicating antioxidative stress properties for PGB (Fig. 2C). Next, RGCs were localized, and the mitochondrial ultrastructure of each group was analyzed. Transmission electron microscopy showed alterations in RGC mitochondrial structure in the RIR-treated retina, including mitochondrial swelling, vacuolization, disintegrated cristae, and increased matrix density, whereas PGB pretreatment improved the mitochondrial structure (Fig. 2D). Collectively, these data suggest that PGB can ameliorate RIR-induced apoptosis through the mitochondrial apoptosis pathway.

PGB Pretreatment Rescued Retinal Visual Dysfunction Through the Alleviation of RGC Disturbance

Retinal function was assessed 7 days after RIR injury using ERG, a noninvasive visual function analysis tool. Amplitude

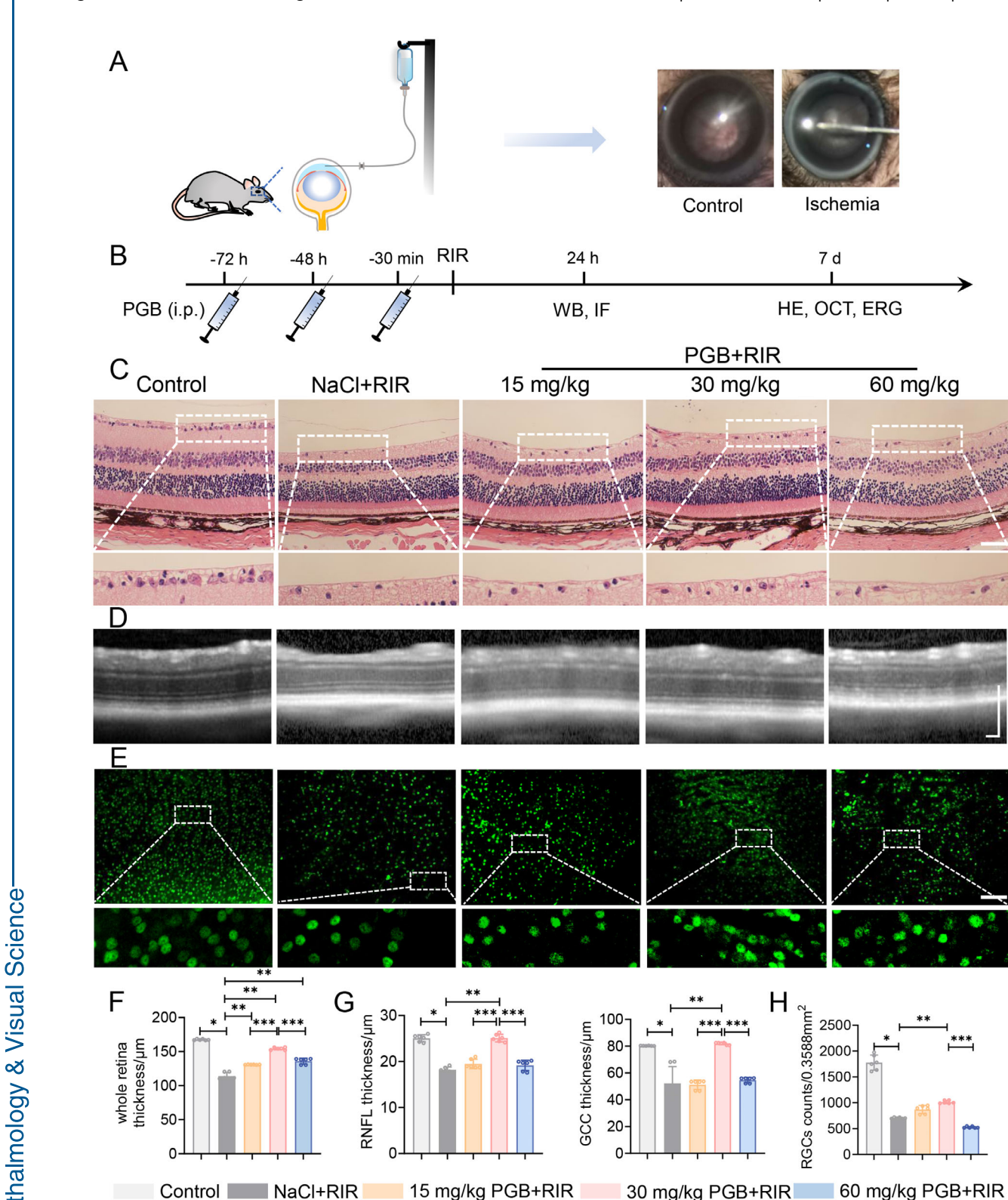


FIGURE 1. PGB performed neuroprotective effects during RIR injury. **(A)** A mouse RIR model was successfully established. Microscopic examination showed that the fundus of normal mice had clear optic disc boundaries and well-filled blood vessels; however, in the ischemic group of mice, which showed a sharp increase in IOP, the retinal optic disc boundaries were unclear, blood vessels were cut off, and the retina appeared pale. **(B)** The mice were pretreated with PGB before modeling, and the neuroprotective effect was evaluated at 24 hours and 7 days after RIR. **(C)** Representative H&E images of retinal sections ($40\times$). Scale bars: 50 μm . **(D)** Representative OCT scans in living mice. Scale bars: 200 μm . **(E)** Representative retinal mounts with fluorescent staining of RGCs ($20\times$). Scale bars: 100 μm . **(F–H)** Thickness of the whole retina (**F**) and RNFL and GCC (**G**) and the number of RGCs (**H**) decreased under RIR insult, whereas PGB pretreatment rescued the deterioration of the above indicators. The most significant improvement was observed at the dose of 30 mg/kg ($n = 6$). * $P < 0.05$ versus control group; ** $P < 0.05$ versus NaCl + RIR group; *** $P < 0.05$ versus 30-mg/kg PGB + RIR group.

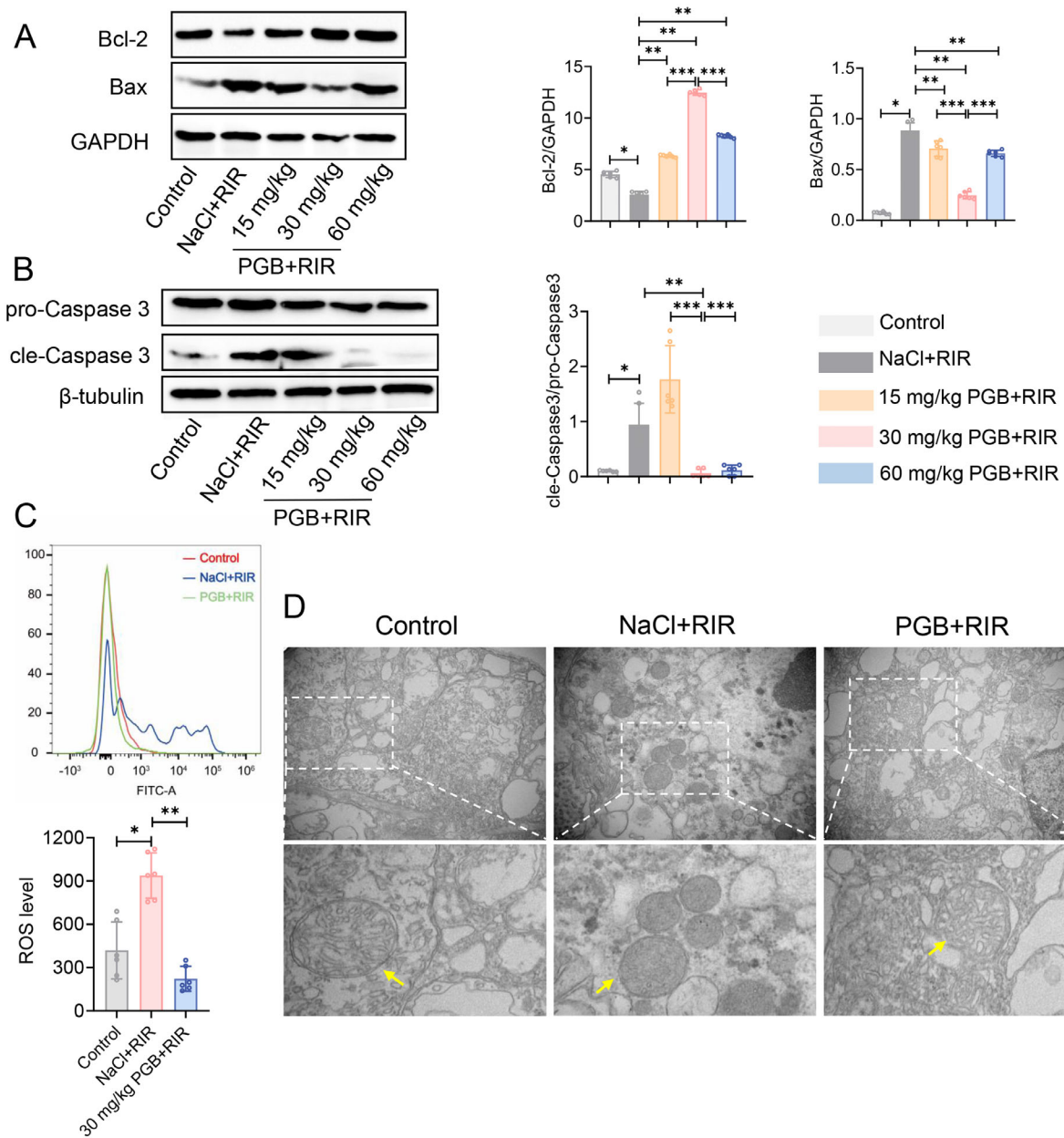


FIGURE 2. PGB reduced mitochondria-associated RGC apoptosis induced by RIR injury. **(A)** PGB pretreatment decreased the expression of pro-apoptotic protein Bax but increased Bcl-2 expression, and the most significant improvement was observed at 30 mg/kg. **(B)** PGB pretreatment reversed the elevation of cleaved caspase 3/pro-caspase 3 elicited by RIR, and the most significant improvement was observed at 30 mg/kg. **(C)** PGB (30 mg/kg) pretreatment inhibited ROS generation. **(D)** RIR injury induced disintegrated cristae and increased matrix density in mitochondria. PGB pretreatment improved the structure of mitochondria following RIR; mitochondria are indicated by the yellow arrow ($n = 6$; 25,000 \times). Scale bars: 500 nm. * $P < 0.05$ versus control group; ** $P < 0.05$ versus NaCl + RIR group; *** $P < 0.05$ versus 30-mg/kg PGB + RIR group.

changes recorded by ERG are thought to reflect the damage of rapid fluctuations in IOP to the inner retina, especially RGC function.²⁵ The average value of the amplitudes of OPs, extracted from the scotopic responses elicited by a light intensity of 3.0 cd·s/m², was lower in the RIR-treated retina versus control by 10.56 ± 1.85 μ V but higher in the PGB pretreated retina by 5.71 ± 1.35 μ V (Fig. 3B). Next, the PhNR was analyzed at a light intensity of 10.0 cd·s/m² under bright adaptation, and the results showed a decrease of 13.32 ± 1.27 μ V after RIR. However, PGB pretreatment restored the amplitudes of PhNRs, with an increase of 11.97 ± 4.68 μ V (Fig. 3C). Moreover, the amplitudes of a- and b-waves were

significantly decreased after RIR injury, but PGB pretreatment failed to rescue the amplitude (Supplementary Data S8).

PGB Conferred Neuroprotection by Mediating the Akt/GSK3 β / β -Catenin Signaling Pathway

The above results showed that PGB could alleviate mitochondria-driven RGC apoptosis and thus prevent retinal neurodegeneration. We further investigated the underlying mechanism of the above effect by examining the

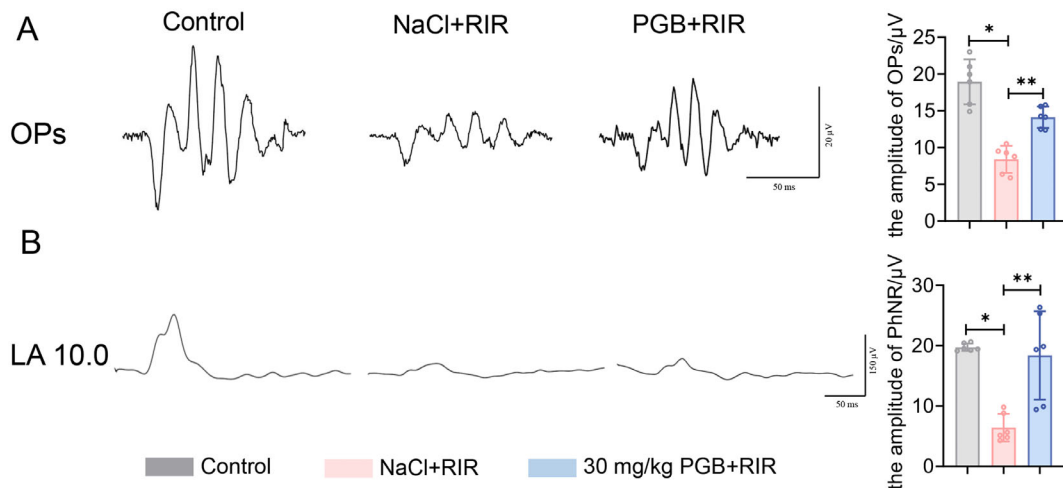


FIGURE 3. PGB improved visual function in the retina of RIR mice models. **(A)** Averaged data of OP amplitudes from recordings obtained 7 days after RIR. **(B)** Averaged data for PhNR amplitudes from recordings obtained 7 days after RIR. The amplitudes of OPs and PhNRs were decreased after RIR, whereas 30-mg/kg PGB pretreatment restored levels of these indicators ($n = 6$). * $P < 0.05$ versus control group; ** $P < 0.05$ versus NaCl + RIR group.

Akt/GSK3 β / β -catenin signaling pathway. A previous study documented that abnormal GSK3 β activation contributes to mitochondrial dysregulation in diabetic retinal neurodegeneration by inhibiting downstream β -catenin-regulated oxidative stress resistance.²⁶ In this study, we found a significant decrease in the phosphorylation of Akt (serine 473) and GSK3 β (serine 9) in the retina following RIR (Fig. 4A), resulting in abnormal activation of GSK3 β (Fig. 4C). Moreover, we examined the levels of β -catenin (a downstream target of GSK3 β) and found that RIR downregulated the expression of β -catenin (Fig. 4A). However, intraperitoneal PGB pretreatment reversed the effects of RIR and restored the high expression of p-Akt, p-GSK3 β , and β -catenin in the RIR-treated retina (Fig. 4A). Furthermore, IF staining was conducted to detect the expression of p-Akt, p-GSK3 β , and β -catenin in RGCs in the ganglion cell layer (GCL). Consistent with previous western blot (WB) results, PGB pretreatment significantly reversed the inhibited expression of p-Akt, p-GSK3 β , and β -catenin in RGCs caused by RIR (Figs. 4B, 4D).

To further validate the role of the Akt/GSK3 β / β -catenin signaling on the protective effects of PGB, MK2206 (10 nM; Selleck Chemicals, Houston, TX, USA),²⁷ an inhibitor of Akt, was intravitreally injected 24 hours prior to RIR to block the activation of Akt caused by PGB. As demonstrated by the WB and IF staining results (Figs. 5A–5D), MK2206 inhibited the phosphorylation of Akt and GSK3 β stimulated by PGB. Moreover, the inactivation of GSK3 β (Fig. 5E) by a specific GSK3 β inhibitor, TWS119 (10 nM; Selleck Chemicals),⁵ significantly enhanced the expression of β -catenin (Fig. 5F). Taken together, our data demonstrated that PGB exerts its neuroprotective effects by promoting the phosphorylation of Akt, inhibiting the activity of GSK3 β and thus mobilizing β -catenin.

PGB Pretreatment Prevents Mitochondrial Impairment and Retinal Dysfunction by Activation of Akt and Inactivation of GSK3 β

β -Catenin is a key mediator of cell survival, and our previous study found that PGB pretreatment could activate Akt and

inhibit GSK3 β .²⁶ We further evaluated the role of Akt/GSK3 β in mitochondrial impairment and retinal visual function. As shown in Figures 6B and 6D, PGB rescued the decrease in RNFL and GCC thickness induced by RIR injury; however, MK2206 reversed the effects of PGB and decreased the RNFL and GCC thickness. Similar results were observed in whole retina thickness by OCT (Supplementary Data S6B). Consistent with these results, PGB increased the amplitudes of OPs and PhNRs following RIR, whereas MK2206 abolished the visual function balance of RGCs in the presence of PGB (Figs. 6C, 6E). Contrasting results were revealed in the retina treated with TWS119. Mice intravitreally injected with TWS119 showed an improved structure of mitochondria and restoration of retinal thickness, as well as an enhanced visual response (Figs. 6A–6E). Collectively, the neuroprotective effects of Akt activation and GSK3 β inhibition were attributed to the upregulated levels of active β -catenin protein (Fig. 5F).

PGB Protects Primary RGCs From OGD/R Injury Via the Akt/GSK3 β / β -Catenin Pathway

Considering the heterogeneity of cell types in the neural retina, we further explored the role of Akt/GSK3 β / β -catenin in OGD/R-induced RGC injury in vitro. Primary cultured RGCs were identified by double immunostaining for RGC-characteristic marker Brn3a (red) and neuronal marker TuJ1 (green), and the ratio of Brn3a $^+$ TuJ1 $^+$ cells was more than 85% (Fig. 7A, Supplementary Data S9). Primary cultured RGCs were exposed to OGD insult for 3 hours and reoxygenated for 12 hours to mimic IOP-triggered RIR damage in vitro. Cell viability was detected by the CCK8 assay. We found that OGD/R induced a significant decrease in cell viability, whereas PGB improved cell viability in a dose-dependent manner, with the most significant improvement observed at 100 μ M (Fig. 7B).^{28,29}

In accordance with the in vivo results, there was a remarkable decrease in Akt and GSK3 β phosphorylation in RGCs upon OGD/R insult (Fig. 7E), accompanied by a significant decrease in β -catenin expression (Fig. 7E) and increased ROS production compared to control cells

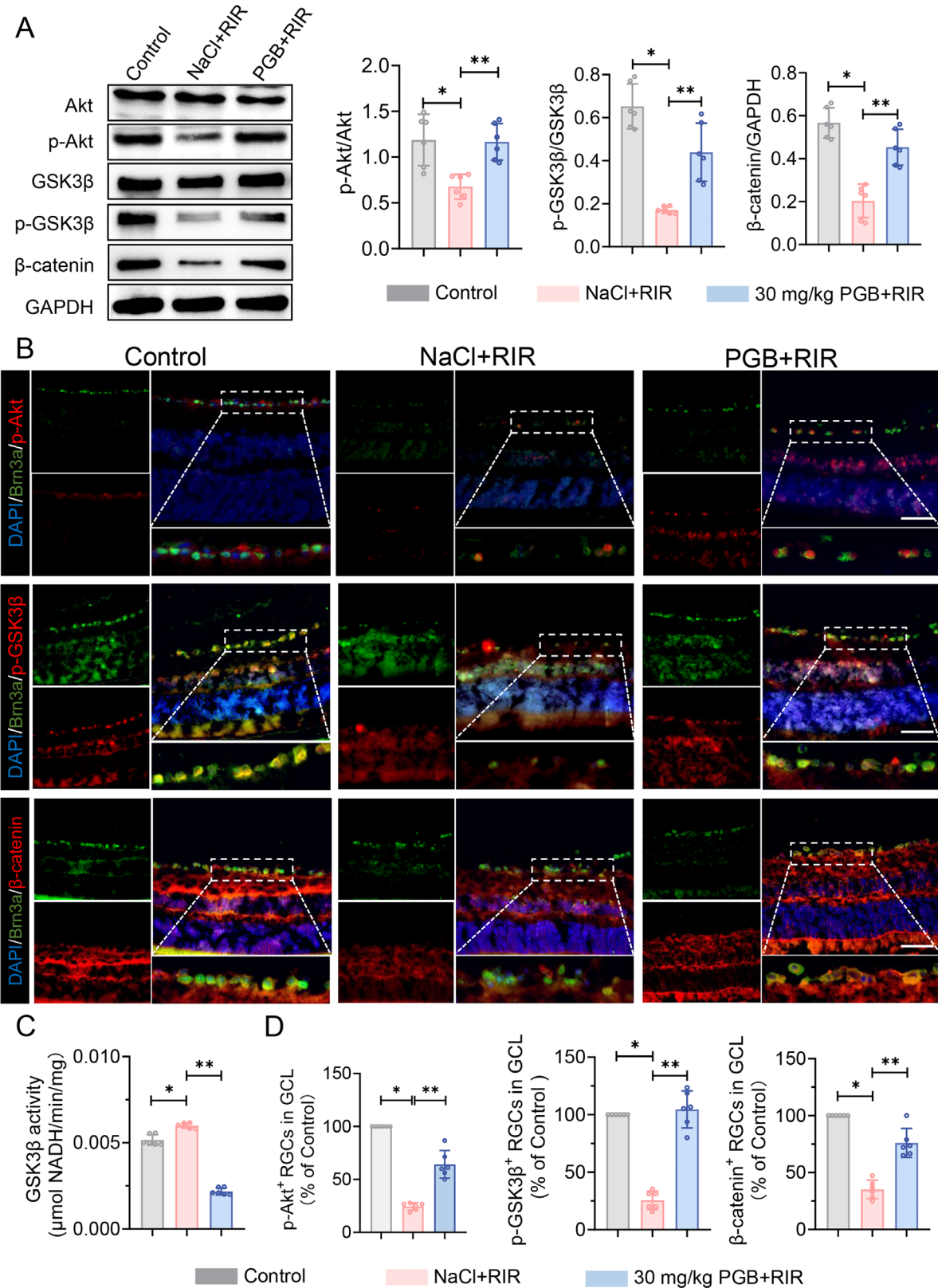


FIGURE 4. PGB protected against RIR injury via the Akt/GSK3 β / β -catenin pathway. **(A)** The results of WB showed that the expression of p-Akt, p-GSK3 β , and β -catenin was downregulated after RIR, whereas PGB (30 mg/kg) pretreatment reversed these findings. **(B, D)** Representative IF images of retinal sections (40 \times). Scale bars: 50 μm . The ratios of RGCs in the GCL expressing p-Akt, p-GSK3 β , and β -catenin were downregulated after RIR, but PGB pretreatment upregulated the proportion of positive cells. **(C)** PGB pretreatment inhibited the activity of GSK3 β ($n = 6$). $^*P < 0.05$ versus control group; $^{**}P < 0.05$ versus NaCl + RIR group.

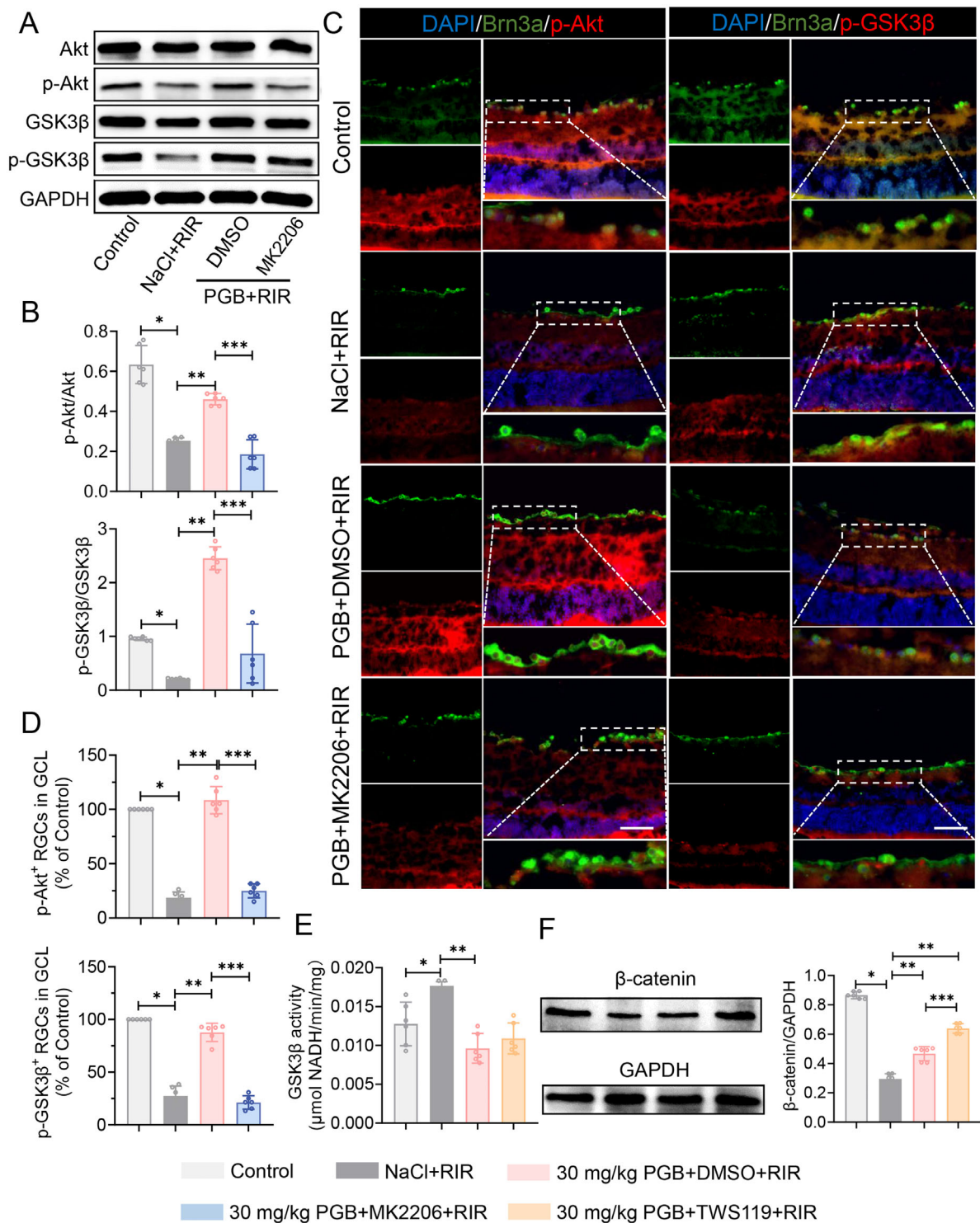


FIGURE 5. The neuroprotective effect of PGB required the phosphorylation of Akt and inactivation of GSK3 β . **(A, B)** The results of WB showed that MK2206 (10 nM) inhibited the phosphorylation of Akt and GSK3 β stimulated by PGB. **(C, D)** Representative IF images of retinal sections (40 \times). Scale bars: 50 μm . MK2206 inhibited the increase in the ratio of RGCs, with p-Akt⁺ and p-GSK3 β ⁺ stimulated by PGB (30 mg/kg). **(E)** Consistent with the effect of PGB pretreatment, TWS119 (10 nM) inhibited the activity of GSK3 β . **(F)** WB showed that TWS119 enhanced the expression of β -catenin ($n = 6$). * $P < 0.05$ versus control group; ** $P < 0.05$ versus NaCl + RIR group; *** $P < 0.05$ versus 30-mg/kg PGB + dimethyl sulfoxide (DMSO) + RIR group.

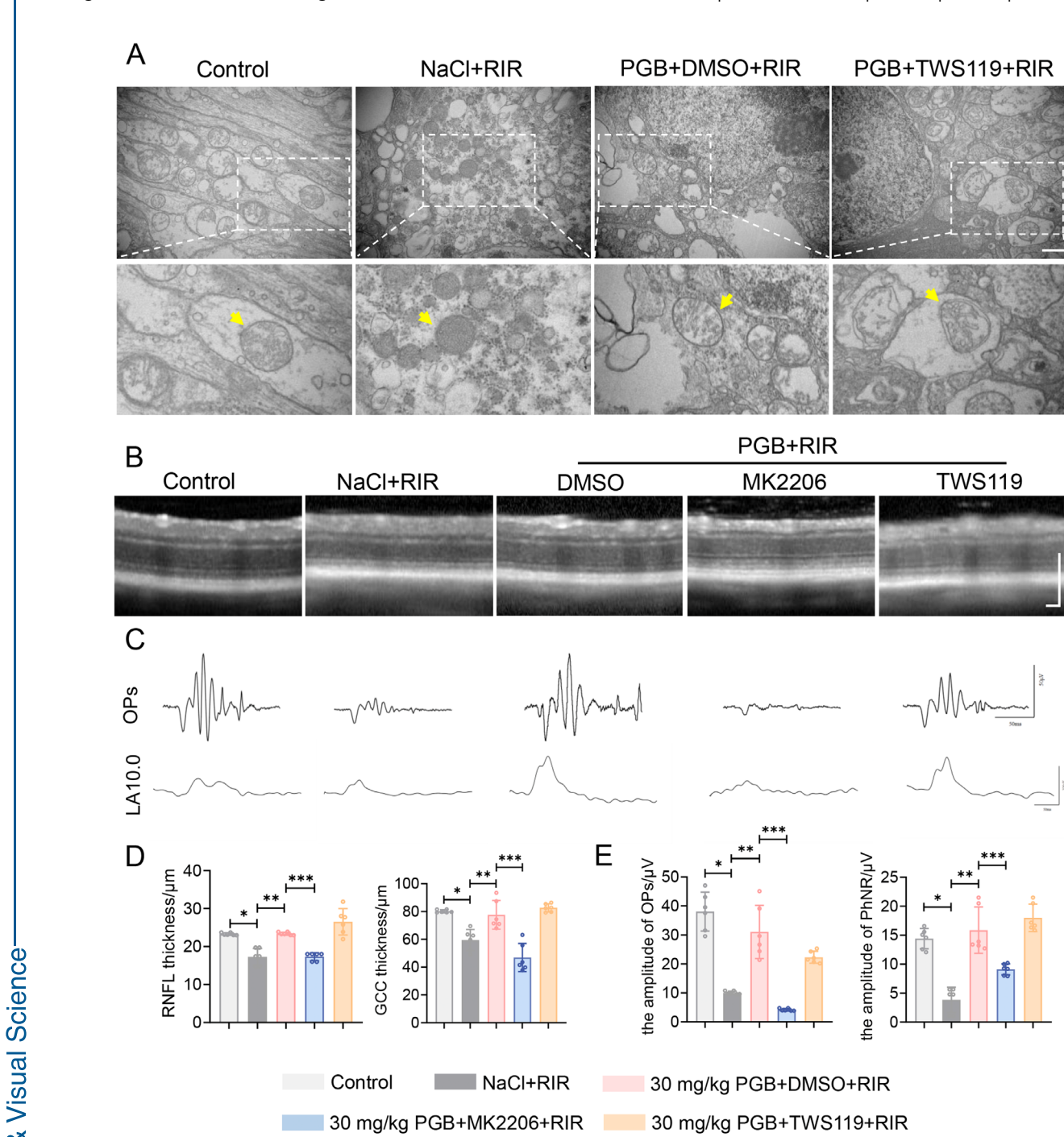


FIGURE 6. PGB pretreatment prevented mitochondrial impairment and retinal dysfunction by the phosphorylation of Akt and inactivation of GSK3 β . **(A)** PGB (30 mg/kg) and TWS119 (10 nM) pretreatment improved the structure of mitochondria in the retina of RIR mice models; mitochondria are indicated by the yellow arrow (25,000 \times). Scale bars: 500 nm. **(B, D)** MK2206 (10 nM) reversed the effects of PGB and decreased the thickness of the RNFL and GCC, and TWS119 maintained the effects of PGB and reserved the increased thickness of RNFL and GCC. Scale bars: 200 μm . **(C, E)** Representative ERG waveforms in living mice. MK2206 disrupted the visual function balance of RGCs in the presence of PGB, with a decrease in the amplitudes of OPs and PhNRs. However, TWS119 maintained the normal level of the amplitudes of OPs and PhNRs ($n = 6$). * $P < 0.05$ versus control group; ** $P < 0.05$ versus NaCl + RIR group; *** $P < 0.05$ versus 30-mg/kg PGB + DMSO + RIR group.

(Fig. 7C). However, PGB pretreatment increased Akt and GSK3 β phosphorylation, thereby increasing β -catenin expression and reducing the ROS level. To further confirm the role of the Akt/GSK3 β / β -catenin pathway in PGB-mediated neuroprotection of RGCs, MK2206 (5 μM) was used to inhibit Akt activity.³⁰ Our results substantiate that

MK2206 treatment counteracts PGB-mediated neuroprotection of RGCs to a certain extent. The reduction in intracellular ROS and increase in the expression of p-Akt, p-GSK3 β , and β -catenin induced by PGB were inhibited to a certain extent by MK2206 (Figs. 7C–7E). Taken together, our findings demonstrate that PGB confers neuroprotection to RGCs

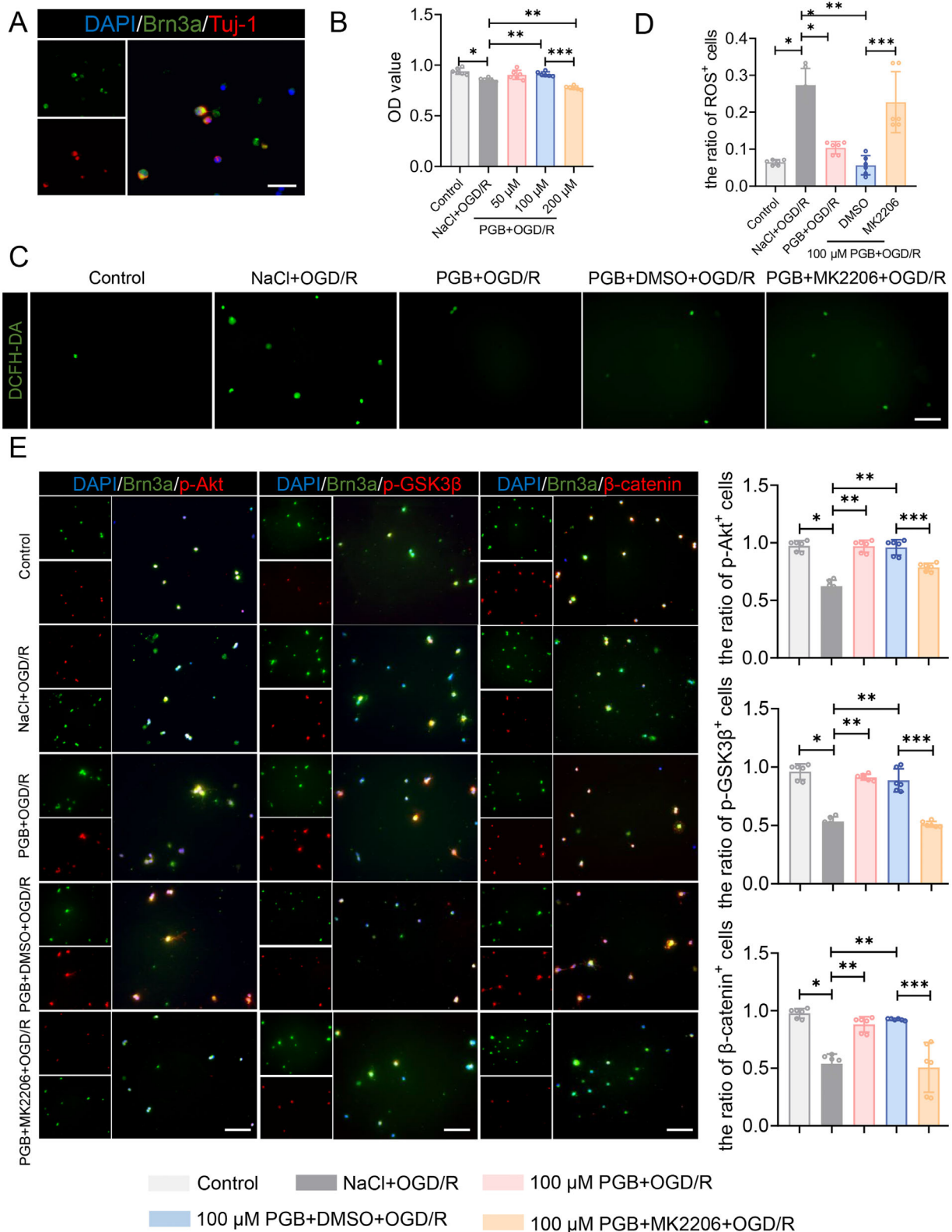


FIGURE 7. PGB protected primary RGCs from OGD/R injury via the Akt/GSK3 β /β-catenin pathway. **(A)** IF identification of primary mice RGCs (40 \times). Scale bars: 50 μ m. **(B)** Primary RGCs pretreated with PGB (50 μ M, 100 μ M, or 200 μ M) for 24 hours were subjected to OGD/R. OGD/R induced a considerable decrease in cell viability, whereas PGB improved cell viability. The most significant improvement was observed at 100 μ M. **(C, D)** Primary RGCs pretreated with MK2206 (5 μ M) were treated with PGB (100 μ M) for 24 hours prior to the onset of OGD/R. The ROS level was measured through the fluorescent probe, DCFH-DA, and the ratio of ROS⁺ cells was measured. PGB pretreatment inhibited ROS generation, but MK2206 counteracted the effect. (40 \times). Scale bars: 50 μ m. **(E)** Representative IF images of primary RGCs (40 \times). Scale bars: 50 μ m. The ratios of RGCs expressing p-Akt, p-GSK3 β , and β-catenin were downregulated after OGD/R, which was countered by PGB pretreatment. However, MK2206 decreased the ratios of positive cells ($n = 6$). * $P < 0.05$ versus control group; ** $P < 0.05$ versus NaCl + OGD/R group; *** $P < 0.05$ versus PGB 100 μ M + OGD/R group; **** $P < 0.05$ versus PGB + DMSO + OGD/R group.

through an Akt/GSK3 β / β -catenin-dependent mechanism in vitro.

DISCUSSION

Glaucoma is a leading cause of blindness worldwide. RIR injury caused by rapid fluctuations in IOP is mainly responsible for the progressive loss of RGCs, the earliest step of neuroretinal degeneration in glaucoma.³¹ Accordingly, identifying vital molecular events and selecting effective drugs to prevent RGC apoptosis in RIR-induced retinal injury is vital for arresting disease development. The present study demonstrated that pretreatment with PGB significantly improved RIR-induced RGC apoptosis and retinal dysfunction via suppressing ROS production and mitochondrial disturbance. Mechanistically, the neuroprotective effects could be attributed to the Akt/GSK3 β / β -catenin pathway activation.

Compared with the previous generation of structural analogs such as gabapentin, PGB brings more advantages in terms of pharmacodynamics and pharmacokinetics, including a stronger ability to bind calcium channels, a lower effective dose, and fewer side effects.^{32,33} The unique pharmacological properties of PGB enhance its efficacy, enabling it to reach a peak concentration in less than 2 hours.³⁴ PGB is currently administered to treat neuropathic pain, especially during late disease stages. However, recent studies have revealed that PGB might also be beneficial in early disease phases by preventing neuronal damage due to long-lasting Ca²⁺ overload,³⁵ indicating the potential of repurposing PGB for treatment in early stages of neurodegenerative diseases. Another study regarding diabetic retinopathy confirmed the neuroprotective effect of PGB by effectively inhibiting retinal glutamate, glial cell activation, and inflammatory burden.¹⁵ Due to its non-negligible neuroprotective efficacy and proven safety, PGB could be a promising candidate for treating glaucoma and other related ocular diseases.

The mouse model of RIR is a well-established in vivo model used to mimic RIR injury. It has been established that the RIR model did produce whole retinal ischemia, damaging multiple cells within the retina.^{36,37} The retina exhibits a regionalized sensitivity to ischemia, with the outer layers being less sensitive than the inner layers.³⁷ Reports often focus on inner retinal neuronal injury, as this paradigm is often used to mimic glaucomatous retinopathy.³⁸ We found that PGB helped maintain a relatively normal morphology of the inner retina and preserve inner retinal neuron populations during RIR. In the present study, we used ERG to evaluate visual function, given that the ERG components OPs and PhNRs can reflect RGC function.³⁹ The reduction in ERG amplitudes was positively correlated with the loss of RGCs after RIR injury, representing the loss of electrophysiological function of RGCs in the retina.⁴⁰ Interestingly, PGB almost completely corrected these RGC-sensitive components but showed partial recovery of a- and b-waves, indicating stronger neuronal plasticity of the inner retina. Recent studies using the specific deletion of 50% of rods, cones, or rod bipolar cells during development or in mature mice have revealed homeostatic plasticity associated with the enhanced ganglion cell responses and maintenance of normal retinal output.^{41,42} Collectively, our data provide compelling evidence that PGB can effectively improve retinal dysfunction in RIR mice, especially in the inner retina.

Current evidence suggests that apoptosis is the primary mechanism in ischemia/reperfusion-associated retinal

degeneration.^{43,44} H&E staining and OCT results combined with quantitative data of neuron-labeled positive cells suggest that the loss of RGCs accounted for the damage to the inner retina. Quantification of apoptosis-related proteins by WB and TUNEL-positive RGCs (Supplementary Data S10) by TUNEL staining further substantiated the apoptosis of RGCs, consistent with the literature.⁴⁵ Meanwhile, ROS production and mitochondrial structural disturbance were also observed. We quantified several key proteins in the mitochondrial apoptosis pathway to further investigate the underlying mechanisms. The Bcl-2 family represents the first documented apoptosis-associated protein family and plays a pivotal role in mediating mitochondrial apoptosis.⁴⁶ Maes et al.⁶ clarified that Bcl-2 and Bax were major regulators of the endogenous caspase-3-dependent apoptosis pathway, determining the fate of neurons. Caspase-3 was documented as one of the leading apoptotic enforcers in the inner layers of the rodent retina during RIR.⁴⁷ In this study, we found that the expression of active cleaved caspase-3 and Bax increased but Bcl-2 decreased in the retina of the RIR mice model. However, these deleterious effects were minimized in the PGB-pretreated RIR mice models. Ali et al.¹⁵ reported that downregulated caspase-3 activity significantly decreased apoptosis of RGCs in diabetic retinopathy after PGB administration. We found that both the ratio of cleaved caspase-3 to caspase-3 and the expression of Bax were reduced, and Bcl-2 expression increased following PGB pretreatment. Therefore, our study identified the mechanism underlying the neuroprotective effect of PGB on mitochondria-driven apoptosis of RGCs.

An increasing body of evidence suggests that the Akt/GSK3 β / β -catenin signaling pathway is essential in maintaining cell survival after ischemic retinal injury.^{48,49} Enhanced phosphorylation at serine 473 in Akt reduced the neuronal death of experimental RIR mice, and inhibition of Akt phosphorylation promoted neuronal damage.⁵⁰ In the present study, we found that PGB significantly enhanced the phosphorylation of Akt following RIR. Generally, p-Akt was maintained at relatively high levels in normal and stable cells.⁵¹ However, the phosphorylation of Akt decreased significantly following RIR injury, whereas PGB promoted the phosphorylation of Akt. In line with these findings, our in vitro study showed that p-Akt expression in the RGCs decreased after OGD/R exposure, and PGB pretreatment increased the levels of p-Akt. Moreover, activated Akt attenuated GSK3 β activity by promoting the phosphorylation of GSK3 β at serine 9. Substantial evidence suggests that inhibition of GSK3 β yields neuroprotective effects in animals with diabetic retinal neurodegeneration.⁵² In the present study, we found that p-GSK3 β expression in GCL decreased after induction of RIR, whereas it was enhanced in PGB-pretreated mice.

Multiple pathways mediate the anti-apoptotic effect of p-GSK3 β . Specifically, the phosphorylation of GSK3 β has been reported to promote cell survival by activating antioxidant activity and inhibiting intracellular ROS accumulation.⁵³ Meanwhile, p-GSK3 β plays a key role in maintaining mitochondrial homeostasis.⁵⁴ Moreover, it has been shown that ischemia/reperfusion could activate Bax, whereas inactive GSK3 β effectively reduced the activation of Bax and its translocation to the mitochondria, thus reducing apoptosis.^{52,55} Furthermore, β -catenin was a downstream substrate of GSK3 β , and activated GSK3 β could enhance the phosphorylation and proteasomal degradation of β -catenin, subsequently leading to cellular apoptosis.⁵⁶ GSK3 β

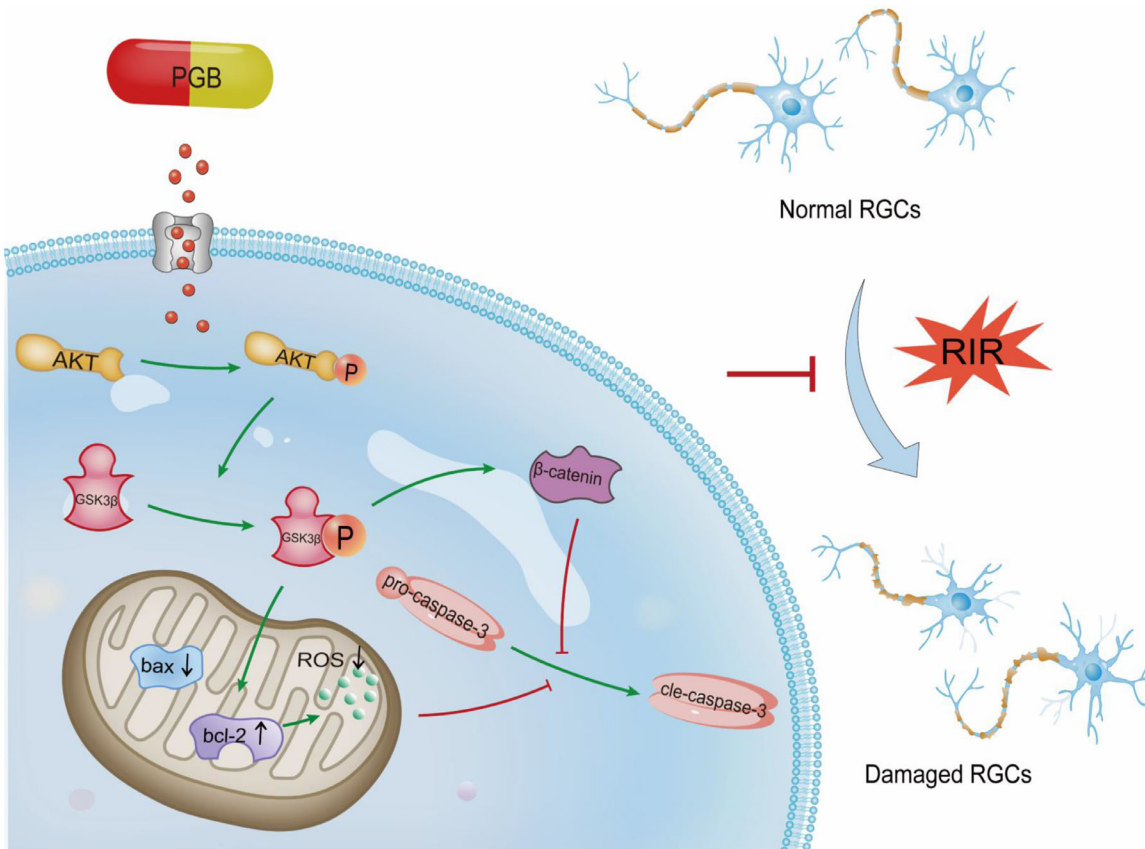


FIGURE 8. PGB enhanced RGC survival following RIR injury via the Akt/GSK3 β /β-catenin signaling pathway.

inhibition increased the level of β-catenin, which favored functional recovery from retinal degeneration.^{26,57} Interestingly, the protein expression of β-catenin increased significantly after the co-inhibition of GSK3 β activity by PGB and TWS119, but no significant differences in OCT and ERG amplitudes were revealed, suggesting that GSK3 β amplified its effect on β-catenin through other intermediate signals. However, the elevated expression of β-catenin could not completely account for the retinal structure and visual function recovery. These findings indicate that GSK3 β accounts predominantly for the neuroprotective effect of PGB, and more research is warranted to explore the underlying mechanisms. In the present study, we found compelling evidence that pretreatment with PGB activates the Akt/GSK3 β signaling pathway and increases the level of β-catenin in retinal tissue following RIR injury. However, it has been shown that Akt could directly phosphorylate β-catenin at serine 552, enhancing its transcriptional activity in the nucleus.^{58,59} Therefore, the effect of Akt on β-catenin phosphorylation in PGB pretreated neural cells remains largely unknown, warranting further investigation.

In conclusion, our study preliminarily validated the neuroprotective effects of PGB in experimental RIR injury, preserving inner retinal neurons and ameliorating retinal morphology and visual function. Our results corroborated that PGB effectively inhibited RGC apoptosis, by inhibiting Bax/Bcl-2 signaling-associated mitochondrial disturbance. More importantly, we identified the potential mechanisms of Akt/GSK3 β /β-catenin pathway activation (Fig. 8). These findings provide compelling evidence that PGB could mediate RGC survival and has great prospects for application in treating RIR injury during glaucoma.

Acknowledgments

The authors thank Yang Hui for her technical support.

Supported by grants from the Science and Technology Planning Project of Guangdong, China (2017A02021100); Science and Technology Program of Guangzhou, China (202102020527); President Foundation of Nanfang Hospital, Southern Medical University (2020C008, 2019Z017, 2021B024); and Medical Scientific Research Foundation of Guangdong, China (A2020325).

Disclosure: J. Xu, None; Y. Guo, None; Q. Liu, None; H. Yang, None; M. Ma, None; J. Yu, None; L. Chen, None; C. Ou, None; X. Liu, None; J. Wu, None

References

- Tham YC, Li X, Wong TY, Quigley HA, Aung T, Cheng CY. Global prevalence of glaucoma and projections of glaucoma burden through 2040: a systematic review and meta-analysis. *Ophthalmology*. 2014;121(11):2081–2090.
- Jonas JB, Aung T, Bourne RR, Bron AM, Ritch R, Panda-Jonas S. Glaucoma. *Lancet*. 2017;390(10108):2183–2193.
- Chan PP, Pang JC, Tham CC. Acute primary angle closure-treatment strategies, evidences and economical considerations. *Eye (Lond)*. 2019;33(1):110–119.
- Boia R, Vecino CE, Santiago AR. Neuroprotective strategies for retinal ganglion cell degeneration: current status and challenges ahead. *Int J Mol Sci*. 2020;21(7):2262.
- Zhu H, Zhang W, Zhao Y, et al. GSK3beta-mediated tau hyperphosphorylation triggers diabetic retinal neurodegeneration by disrupting synaptic and mitochondrial functions. *Mol Neurodegener*. 2018;13(1):62.

6. Maes ME, Schlamp CL, Nickells RW. BAX to basics: how the BCL2 gene family controls the death of retinal ganglion cells. *Prog Retin Eye Res.* 2017;57:1–25.
7. Williams PA, Harder JM, Foxworth NE, et al. Vitamin B3 modulates mitochondrial vulnerability and prevents glaucoma in aged mice. *Science.* 2017;355(6326):756–760.
8. Musayeva A, Unkrig JC, Zhudtseva MB, et al. Betulinic acid protects from ischemia-reperfusion injury in the mouse retina. *Cells.* 2021;10(9):2440.
9. Zhou X, Lv J, Li G, et al. Rescue the retina after the ischemic injury by polymer-mediated intracellular superoxide dismutase delivery. *Biomaterials.* 2021;268:120600.
10. Luo H, Zhuang J, Hu P, et al. Resveratrol delays retinal ganglion cell loss and attenuates gliosis-related inflammation from ischemia-reperfusion injury. *Invest Ophthalmol Vis Sci.* 2018;59(10):3879–3888.
11. Derry S, Bell RF, Straube S, Wiffen PJ, Aldington D, Moore RA. Pregabalin for neuropathic pain in adults. *Cochrane Database Syst Rev.* 2019;1(1):CD007076.
12. Stahl SM, Porreca F, Taylor CP, Cheung R, Thorpe AJ, Clair A. The diverse therapeutic actions of pregabalin: is a single mechanism responsible for several pharmacological activities? *Trends Pharmacol Sci.* 2013;34(6):332–339.
13. Li Z, Taylor CP, Weber M, et al. Pregabalin is a potent and selective ligand for $\alpha(2)\delta$ -1 and $\alpha(2)\delta$ -2 calcium channel subunits. *Eur J Pharmacol.* 2011;667(1–3):80–90.
14. Alles SRA, Cain SM, Snutch TP. Pregabalin as a pain therapeutic: beyond calcium channels. *Front Cell Neurosci.* 2020;14:83.
15. Ali SA, Zaitone SA, Dessouki AA, Ali AA. Pregabalin affords retinal neuroprotection in diabetic rats: suppression of retinal glutamate, microglia cell expression and apoptotic cell death. *Exp Eye Res.* 2019;184:78–90.
16. Koellhoffer EC, McCullough LD. The effects of estrogen in ischemic stroke. *Transl Stroke Res.* 2013;4(4):390–401.
17. Chen H, Deng Y, Gan X, et al. NLRP12 collaborates with NLRP3 and NLRC4 to promote pyroptosis inducing ganglion cell death of acute glaucoma. *Mol Neurodegener.* 2020;15(1):26.
18. Boia R, Salinas Navarro M, Gallego Ortega A, et al. Activation of adenosine A3 receptor protects retinal ganglion cells from degeneration induced by ocular hypertension. *Cell Death Dis.* 2020;11(5):401.
19. Winzeler A, Wang JT. Purification and culture of retinal ganglion cells from rodents. *Cold Spring Harb Protoc.* 2013;2013(7):643–652.
20. Wan P, Su W, Zhang Y, et al. LncRNA H19 initiates microglial pyroptosis and neuronal death in retinal ischemia/reperfusion injury. *Cell Death Differ.* 2020;27(1):176–191.
21. Boudie L, Mountadem S, Lashermes A, et al. Blocking $\alpha 2\delta$ -1 subunit reduces bladder hypersensitivity and inflammation in a cystitis mouse model by decreasing NF- κ B pathway activation. *Front Pharmacol.* 2019;10:133.
22. Elgazzar FM, Elseady WS, Hafez AS. Neurotoxic effects of pregabalin dependence on the brain frontal cortex in adult male albino rats. *Neurotoxicology.* 2021;83:146–155.
23. Daneshdoust D, Khalili-Fomeshi M, Ghasemi-Kasman M, et al. Pregabalin enhances myelin repair and attenuates glial activation in lysolecithin-induced demyelination model of rat optic chiasm. *Neuroscience.* 2017;344:148–156.
24. Amorim JA, Coppotelli G, Rolo AP, Palmeira CM, Ross JM, Sinclair DA. Mitochondrial and metabolic dysfunction in ageing and age-related diseases. *Nat Rev Endocrinol.* 2022;18(4):243–258.
25. Robson AG, Nilsson J, Li S, et al. ISCEV guide to visual electrodiagnostic procedures. *Doc Ophthalmol.* 2018;136(1):1–26.
26. Shu XS, Zhu H, Huang X, et al. Loss of β -catenin via activated GSK3 β causes diabetic retinal neurodegeneration by instigating a vicious cycle of oxidative stress-driven mitochondrial impairment. *Aging (Albany NY).* 2020;12(13):13437–13462.
27. Shu X, Zhang Y, Li M, et al. Topical ocular administration of the GLP-1 receptor agonist liraglutide arrests hyperphosphorylated tau-triggered diabetic retinal neurodegeneration via activation of GLP-1R/Akt/GSK3 β signaling. *Neuropharmacology.* 2019;153:1–12.
28. Baba H, Petrenko AB, Fujiwara N. Clinically relevant concentration of pregabalin has no acute inhibitory effect on excitation of dorsal horn neurons under normal or neuropathic pain conditions: an intracellular calcium-imaging study in spinal cord slices from adult rats. *Brain Res.* 2016;1648(pt A):445–458.
29. Micheva KD, Taylor CP, Smith SJ. Pregabalin reduces the release of synaptic vesicles from cultured hippocampal neurons. *Mol Pharmacol.* 2006;70(2):467–476.
30. Fu P, Wu Q, Hu J, Li T, Gao F. Baclofen protects primary rat retinal ganglion cells from chemical hypoxia-induced apoptosis through the Akt and PERK pathways. *Front Cell Neurosci.* 2016;10:255.
31. Fry LE, Fahy E, Chrysostomou V, et al. The coma in glaucoma: retinal ganglion cell dysfunction and recovery. *Prog Retin Eye Res.* 2018;65:77–92.
32. Field MJ, Cox PJ, Stott E, et al. Identification of the $\alpha 2\delta$ -1 subunit of voltage-dependent calcium channels as a molecular target for pain mediating the analgesic actions of pregabalin. *Proc Natl Acad Sci U S A.* 2006;103(46):17537–17542.
33. Perez C, Latymer M, Almas M, et al. Does duration of neuropathic pain impact the effectiveness of pregabalin? *Pain Pract.* 2017;17(4):470–479.
34. Buvanendran A, Kroin JS, Kari M, Tuman KJ. Can a single dose of 300 mg of pregabalin reach acute antihyperalgesic levels in the central nervous system? *Reg Anesth Pain Med.* 2010;35(6):535–538.
35. Hundehege P, Fernandez-Orth J, Romer P, et al. Targeting voltage-dependent calcium channels with pregabalin exerts a direct neuroprotective effect in an animal model of multiple sclerosis. *Neurosignals.* 2018;26(1):77–93.
36. Hartsock MJ, Cho H, Wu L, Chen WJ, Gong J, Duh EJ. A mouse model of retinal ischemia-reperfusion injury through elevation of intraocular pressure. *J Vis Exp.* 2016;113:54065.
37. Osborne NN, Casson RJ, Wood JP, Chidlow G, Graham M, Melena J. Retinal ischemia: mechanisms of damage and potential therapeutic strategies. *Prog Retin Eye Res.* 2004;23(1):91–147.
38. Luo H, Zhuang J, Hu P, et al. Resveratrol delays retinal ganglion cell loss and attenuates gliosis-related inflammation from ischemia-reperfusion injury. *Invest Ophthalmol Vis Sci.* 2018;59(10):3879–3888.
39. Porciatti V. Electrophysiological assessment of retinal ganglion cell function. *Exp Eye Res.* 2015;141:164–170.
40. Li Z, Xie F, Yang N, et al. Kruppel-like factor 7 protects retinal ganglion cells and promotes functional preservation via activating the Akt pathway after retinal ischemia-reperfusion injury. *Exp Eye Res.* 2021;207:108587.
41. Care RA, Anastassov IA, Kastner DB, Kuo YM, Della SL, Dunn FA. Mature retina compensates functionally for partial loss of rod photoreceptors. *Cell Rep.* 2020;31(10):107730.
42. Shen N, Wang B, Soto F, Kerschensteiner D. Homeostatic plasticity shapes the retinal response to photoreceptor degeneration. *Curr Biol.* 2020; 30(10):1916–1926.
43. Almasieh M, Wilson AM, Morquette B, Cuevas Vargas JL, Di Polo A. The molecular basis of retinal ganglion cell death in glaucoma. *Prog Retin Eye Res.* 2012;31(2):152–181.

44. Ji K, Li Z, Lei Y, et al. Resveratrol attenuates retinal ganglion cell loss in a mouse model of retinal ischemia reperfusion injury via multiple pathways. *Exp Eye Res.* 2021;209:108683.
45. Huang R, Xu Y, Lu X, et al. Melatonin protects inner retinal neurons of newborn mice after hypoxia-ischemia. *J Pineal Res.* 2021;71(1):e12716.
46. Delbridge AR, Grabow S, Strasser A, Vaux DL. Thirty years of BCL-2: translating cell death discoveries into novel cancer therapies. *Nat Rev Cancer.* 2016;16(2):99–109.
47. Thomas CN, Berry M, Logan A, Blanch RJ, Ahmed Z. Caspases in retinal ganglion cell death and axon regeneration. *Cell Death Discov.* 2017;3:17032.
48. Kuo SC, Chio CC, Yeh CH, et al. Mesenchymal stem cell-conditioned medium attenuates the retinal pathology in amyloid-beta-induced rat model of Alzheimer's disease: underlying mechanisms. *Aging Cell.* 2021;20(5):e13340.
49. Wang B, Hu C, Yang X, et al. Inhibition of GSK-3 β activation protects SD rat retina against N-methyl-N-nitrosourea-induced degeneration by modulating the Wnt/ β -catenin signaling pathway. *J Mol Neurosci.* 2017;63(2):233–242.
50. Wang Y, Lopez D, Davey PG, et al. Calpain-1 and calpain-2 play opposite roles in retinal ganglion cell degeneration induced by retinal ischemia/reperfusion injury. *Neurobiol Dis.* 2016;93:121–128.
51. Xu B, Wang T, Xiao J, et al. FCPR03, a novel phosphodiesterase 4 inhibitor, alleviates cerebral ischemia/reperfusion injury through activation of the AKT/GSK3 β / β -catenin signaling pathway. *Biochem Pharmacol.* 2019;163:234–249.
52. Ying Y, Zhang YL, Ma CJ, et al. Neuroprotective effects of ginsenoside Rg1 against hyperphosphorylated tau-induced diabetic retinal neurodegeneration via activation of IRS-1/Akt/GSK3 β signaling. *J Agric Food Chem.* 2019;67(30):8348–8360.
53. Xu B, Xu J, Cai N, et al. Roflumilast prevents ischemic stroke-induced neuronal damage by restricting GSK3 β -mediated oxidative stress and IRE1 α /TRAF2/JNK pathway. *Free Radic Biol Med.* 2021;163:281–296.
54. Liu J, Li L, Xie P, et al. Sevoflurane induced neurotoxicity in neonatal mice links to a GSK3 β /Drp1-dependent mitochondrial fission and apoptosis. *Free Radic Biol Med.* 2022;181:72–81.
55. Guedes JP, Baptista V, Santos-Pereira C, et al. Acetic acid triggers cytochrome *c* release in yeast heterologously expressing human Bax. *Apoptosis.* 2022;27(5–6):368–381.
56. Beurel E, Grieco SF, Jope RS. Glycogen synthase kinase-3 (GSK3): regulation, actions, and diseases. *Pharmacol Ther.* 2015;148:114–131.
57. Rolev KD, Shu XS, Ying Y. Targeted pharmacotherapy against neurodegeneration and neuroinflammation in early diabetic retinopathy. *Neuropharmacology.* 2021;187:108498.
58. Fang D, Hawke D, Zheng Y, et al. Phosphorylation of beta-catenin by AKT promotes beta-catenin transcriptional activity. *J Biol Chem.* 2007;282(15):11221–11229.
59. Gantner BN, Jin H, Qian F, Hay N, He B, Ye RD. The Akt1 isoform is required for optimal IFN- β transcription through direct phosphorylation of β -catenin. *J Immunol.* 2012;189(6):3104–3111.